Joint Reduction of Peak-to-Average Power Ratio, Cubic Metric, and Block Error Rate in OFDM Systems Using Network Coding

Ronny Yongho Kim, *Senior Member, IEEE*, Young Yong Kim, *Member, IEEE*, Amin Alamdar Yazdi, *Student Member, IEEE*, Sameh Sorour, *Student Member, IEEE*, and Shahrokh Valaee, *Senior Member, IEEE*

***Abstract*—The reductions of peak-to-average power ratio (PAPR) and block error rate (BLER) are two challenges in wireless systems employing orthogonal frequency-division multiplexing (OFDM)/orthogonal frequency-division multiple access. High BLER renders the system unreliable, and high PAPR is associated with power inefficiency and nonlinearity of the system. These two issues have separately been studied in the literature, but few works have studied simultaneous reductions of PAPR and BLER. In this paper, we propose a new scheme to jointly reduce and tradeoff PAPR and BLER in OFDM systems using random network coding (NC). In our proposed scheme, different representations of the input information block are generated using a special form of NC matrices, for which we prove it achieves the minimum BLER. We then propose an additional step to our proposed scheme to tradeoff a further improvement in PAPR against degradation in BLER using encoded block puncturing. Simulation results show that the proposed scheme achieves the same PAPR as conventional selective mapping (C-SLM) schemes while achieving the minimum BLER. We also show through simulations the PAPR gains achieved by our proposed additional step over C-SLM and the tradeoff of this gain against BLER degradation. Simulations finally show that our proposed scheme achieves the same results for the recently developed cubic metric.**

***Index Terms*—Cubic metric (CM), multicarrier systems, network coding (NC), peak-to-average power ratio (PAPR), random NC, selective mapping (SLM).**

I. Introduction

MULTICARRIER transmission represents a direction that most state-of-the-art wireless communication standards evolve toward, including digital video broadcasting [2], IEEE 802.11 [3], IEEE 802.16 [4], and 3rd Generation Partnership Project (3GPP) Long Term Evolution (LTE) [5] standards. Multicarrier modulation, such as orthogonal frequency-division multiplexing (OFDM), is a well-known modulation scheme that has proven its efficiency in reliable data communications. Like any other technique, OFDM encounters some challenges, one of which is its high peak-to-average power ratio (PAPR). High PAPR requires a large power backoff in the transmitting amplifier, which translates to low power efficiency. Another metric quantifying the same problem is the cubic metric (CM), which provides a better prediction of the power capability than PAPR. The use of CM, as an evaluation metric, is proposed and adopted in the 3GPP standards [6], [7]. The lower the value of CM, the more efficient the performance of the power amplifier. Reducing the PAPR or CM is a critical issue in portable wireless devices where power is at premium.

Different PAPR reduction approaches were introduced in the literature, which can be partitioned into two main categories: 1) distortion techniques and 2) distortionless techniques. Examples of distortion techniques are clipping [8] and companding [9]. Since distortion-based PAPR reduction schemes would lower the signal-to-noise ratio (SNR) or signal-to-noise-and-distortion ratio, special techniques in transmitter [10] or receiver [11] were studied to minimize the impact of signal distortion. Examples of distortionless techniques are systematic coding [12], selective coding [13], partial transmit sequence [14], tone injection/reservation [15], and active constellation extension [16]. Recently, a distortionless technique called selective mapping (SLM) has attracted much attention because of its effectiveness, strong PAPR reduction capabilities, and low implementation complexities within manageable number of subcarriers [17]–[19].

Another important challenge in wireless networks is reducing the transmission error rate to effectively maximize the achievable throughput, even when unpredictable and time-varying block errors exist. Forward error correction (FEC) technique is employed as a solution to this problem to achieve reliable communications in wireless networks [20]. In the physical layer, various FEC codes, such as convolutional and turbo codes, can be employed. In current wireless communication standards, data streams are divided into source blocks, and

Manuscript received October 26, 2010; revised August 29, 2011; accepted October 4, 2011. Date of publication October 19, 2011; date of current version December 9, 2011. This work was supported by The Ministry of Knowledge Economy (MKE), Korea, under the Information Technology Research Center (ITRC) support program supervised by the National IT Industry Promotion Agency (NIPA) under NIPA-2011-C1090-1111-0006. The review of this paper was coordinated by Prof. H.-H. Chen.

R. Y. Kim is with the School of Computer Engineering, Kyungil University, Gyeongsan 712-701, Korea (e-mail: ronnykim@kiu.ac.kr).

Y. Y. Kim is with the Department of Electrical and Electronic Engineering, Yonsei University, Seoul 120-749, Korea (e-mail: y2k@yonsei.ac.kr).

A. A. Yazdi, S. Sorour, and S. Valaee are with the Department of Electrical and Computer Engineering, University of Toronto, Toronto, ON M5S 3G4, Canada (e-mail: ayazdi@comm.utoronto.ca; samehsorour@comm.utoronto.ca; valaee@comm.utoronto.ca).

Color versions of one or more of the figures in this paper are available online at http://ieeexplore.ieee.org.

Digital Object Identifier 10.1109/TVT.2011.2172698

each of these blocks is passed to a FEC processor to generate coded blocks that are more immune to channel errors. Thus, these coded blocks endure lower block error rates (BLER) when transmitted over channels with unpredictable errors.

As previously stated, a large spectrum of techniques and algorithms have been developed to reduce PAPR and BLER separately. In current OFDM-based networks, the source blocks are generally passed through BLER reduction algorithms; then, the resulting streams are applied to PAPR reduction methods. However, few works have studied the simultaneous reductions of both PAPR and BLER.

In another stream of research, network coding (NC) has originally been proposed in information theory [21], with the objective of maximizing network information flow, and has since emerged as one of the most promising information-theoretic approaches for throughput improvement. In [22], medium access control layer random NC, which is denoted as MRNC, has been introduced to avoid the overhead problems incurred by hybrid automatic repeat request (HARQ). In MRNC, the U packets of a given data frame are linearly combined with random nonzero coefficients, and the resulting coded packets are transmitted. Yazdi *et al.* derived conditions for the minimum packet error rate in wireless channels when NC is employed for error resilience [23]. Katti *et al.* proposed MIXIT [24], a protocol for cooperative packet recovery using symbol-level random NC, which performs opportunistic routing on groups of correctly received symbols in a packet.

Although NC has extensively been studied, and its capability on multicarrier system is anticipated, the idea of employing it for joint PAPR/CM and BLER reduction has not yet been proposed to the best of our knowledge. Consequently, we first propose a new scheme that employs NC to jointly reduce the PAPR/CM and BLER in multicarrier systems. This scheme consists of generating different sets of N coded blocks from a set of K source blocks $(K < N)$ using a special form of NC matrices, which we prove achieves the minimum BLER. After symbol mapping and inverse fast Fourier transform (IFFT) of all these different sets, the signal with the lowest PAPR or CM is selected. In other words, this scheme can be viewed as a network-coded SLM (NC-SLM) scheme that employs specific NC matrices, instead of phase rotations, to generate different representations of the OFDM symbol while minimizing the BLER. Consequently, this scheme is expected to achieve similar PAPR or CM reduction performance to conventional SLM (C-SLM) while achieving the optimal BLER. In addition, this approach is a more general and practically implementable version of our previous work in [1], where a joint reduction of PAPR and symbol loss rate was proposed in a multicarrier system. In contrast to the physical modulation symbol-level NC in [1], we propose in this paper to use block-level NC operation to overcome some limitations incurred by rigid structure using modulation symbol-level operation. In this paper, we refer to a "block" as a group of bits that are much larger and independent of the modulation-level symbols employed in the physical layer.

For further reduction of PAPR or CM, we propose an additional step to our scheme that exploits the addition of redundant coded blocks by NC to puncture some of them. This additional step consists of finding and puncturing the coded blocks that will result in the maximum PAPR or CM reduction. We will refer to this step as the block puncturing step. The execution of this step achieves a better PAPR or CM reduction, compared with C-SLM, at the cost of BLER performance degradation. Consequently, this step can optionally be used to further reduce the PAPR or CM when the first step fails in achieving the target PAPR or CM value.

The rest of this paper is organized as follows. Section II reviews some key concepts that we will employ in this paper, such as PAPR, CM, SLM, symbol-level NC, and block-level NC. The description of the proposed scheme is presented in Section III. The second step of the proposed scheme, i.e., block puncturing, is presented in Section IV. In Section V, we present simulations comparing our proposed scheme with the C-SLM scheme and showing the PAPR-BLER tradeoff through block puncturing. Finally, we conclude this paper in Section VI.

II. Review of Key Concepts

A. PAPR

Let $\underline{s} = [s_1, s_2, \ldots, s_F]$ be a modulated data sequence of length F during the time interval $[0, T]$, where s_i is a symbol from a signal constellation, F is the number of OFDM data subcarriers, and T is the OFDM symbol duration. The complex baseband representation of the transmit signal can thus be formulated as

$$x(t) = \sum_{i=1}^{F} s_i . \exp(j2\pi f_i t), \quad 0 \le t \le T \tag{1}$$

where $j = \sqrt{-1}$. The PAPR of $x(t)$ is defined as

$$PAPR = \frac{\max_{0 \le t \le T} |x(t)|^2}{\frac{1}{T}\int_0^T |x(t)|^2 \, dt}. \tag{2}$$

A major drawback of the PAPR metric is that it does not take into account the secondary peaks of power that considerably affect the power amplifier performance due to the cubic term in the amplifier gain characteristic function defined as [6]

$$x_o(t) = G1 \cdot \left(x_i(t) + G3 \cdot |x_i(t)|^3 \right) \tag{3}$$

where $x_i(t)$ and $x_o(t)$ are the amplifier's input and output voltages, respectively.

B. CM

To get a better prediction (than the PAPR) of the power capability (derating) of a given power amplifier on an input signal, the CM has been adopted by the 3GPP. The CM of a signal is defined as [7]

$$CM = \frac{RCM - RCM_{\text{ref}}}{K_{\text{CM}}} \tag{4}$$

where K_{CM} is an empirical slope factor, RCM is an abbreviation for raw CM, and RCM_{ref} is the raw CM of the wideband

code-division multiple-access voice reference signal. RCM is defined for a signal $x(t)$ as

$$RCM = 20\log\left(RMS\left(\left(\frac{|x(t)|}{RMS\,(x(t))}\right)^3\right)\right) \quad (5)$$

where RMS is the root mean square value. Since RCM_{ref} and K_{CM} are constant values, RCM can be used as a performance metric. In this paper, we use both PAPR and CM as performance metrics.

C. C-SLM

SLM can simply be defined as the process of generating different output representations of the input data sequence to a multicarrier modulator using predefined phase rotation sequences and selecting the representation that achieves the lowest PAPR for transmission. Let $\Phi^{(m)} = [\phi_1^{(m)}, \ldots, \phi_F^{(m)}]$, $1 \le m \le U$, be prefixed phase sequences. Thus, U representations of the modulated data sequence $\underline{s}$ can be obtained as follows:

$$s_i^{(m)} = s_i.e^{j\phi_i^{(m)}}. \quad (6)$$

In other words, $s_i^{(m)}$ is a phase-rotated version of s_i. After applying IFFT to these U versions using (1), their PAPR can be computed using (2), respectively. The C-SLM then selects and transmits the version that achieves the lowest PAPR among these U PAPRs. C-SLM can find the minimum PAPR through exhaustive search of phase factors in a phase sequence. However, since the optimization of C-SLM requires heavy computing complexity as the number of subcarrier increases, the C-SLM scheme originally proposed in [25] is utilized in this paper.

D. Symbol-Level Versus Block-Level NC

Symbol-level NC is performed over symbols at the physical layer. In this paper, we use the term "symbol" to describe the unit of data that is defined by the modulation scheme in the physical layer. For example, one symbol represents 2 bits if quadrature phase shift keying (QPSK) is used and 4 bits if 16 quadrature amplitude modulation (16-QAM) is used. In our previous work [1], symbol-level NC was performed on modulation symbols. In such operation, the size of the NC block is selected to be the same as the number of bits represented by the employed modulation level. Therefore, the coding operations are done using a finite field with dimension related to the employed modulation level. For example, in case of 16-QAM, $GF(2^4)$ is used for the encoding/decoding operation, and a 4-bit block size is selected for efficient and simple finite field operation. One coded block, which represents one modulation symbol, is mapped to one subcarrier.

In this paper, we propose to employ block-level NC operations instead of modulation symbol-based operations. This provides more flexibility and adaptability while still taking the full benefits of modulation symbol-based NC. The main advantages of block-level NC over symbol-level NC are the following:

1) Flexibility: Block and finite field sizes can flexibly be changed since block partitioning can be performed irrespective of modulation. In symbol-level NC, when the modulation scheme is changed due to varying channel conditions, the block and finite field sizes should be changed, which result in performance degradation because blocks encoded with different finite fields cannot be decoded.
2) Adaptability: Since the operating finite field and block size selection do not depend on a given modulation scheme, they can adaptively be selected by taking varying channel conditions into account.

III. Proposed Scheme

In this section, we provide a detailed description of our proposed scheme to jointly reduce PAPR/CM and BLER. The core of this scheme is the NC-SLM approach (instead of C-SLM), in which different NC matrices are used to generate different representations of the OFDM symbol. The employed coding matrices are designed so as to minimize the BLER. For further PAPR or CM reduction, we introduce a block puncturing step, which reduces PAPR or CM at the expense of some BLER performance degradation. The block diagram of the proposed scheme is shown in Fig. 1.

A. Network-Coded Block Generation

At the physical layer, the transmitter divides the input bit stream into blocks with fixed size, each of which contains a certain number of physical layer symbols. Let K be the number of blocks that can be transmitted over one OFDM symbol after block encoding, and let u_i $(i = 1, 2, \ldots, K)$ be the ith block in the OFDM symbol. Let $\underline{\mathbf{u}} = [u_1, u_2, \ldots, u_K]$ be the vector of original blocks in a single OFDM symbol.

After block partitioning, the original block vector $\underline{\mathbf{u}}$ is passed to NC units, each encoding the K blocks of $\underline{\mathbf{u}}$ into N coded blocks $(N > K)$. Let $\mathbf{A}^{(m)} = [a_{ij}^{(m)}]$ $(i \in \{1, \ldots, K\}, j \in \{1, \ldots, N\}, m \in \{1, \ldots, U\})$ be the coding matrix of the mth unit. The elements of $\mathbf{A}^{(m)}$ are chosen from a Galois field, whose size is determined by the number of bits per block (e.g., for a block of 8 bits, GF(2^8) should be used). Each coded block $y_j^{(m)}$, $j \in \{1, \ldots, N\}$, can then be generated as follows:

$$y_j^{(m)} = \sum_{i=1}^{K} u_i a_{ij}^{(m)}. \quad (7)$$

In other words, each coded block is a linear combination of a subset or all of the original data blocks. Consequently, the $1 \times K$ vector of the original blocks is encoded into a $1 \times N$ vector of coded blocks in the mth coding unit as

$$\underline{\mathbf{y}}^{(m)} = \left[y_1^{(m)}, y_2^{(m)}, \ldots, y_N^{(m)}\right] = \underline{\mathbf{u}} \cdot \mathbf{A}^{(m)}. \quad (8)$$

The code rate (r) of this process is $r = (K/N)$. Any K of these coded blocks can be used at the receiver to decode

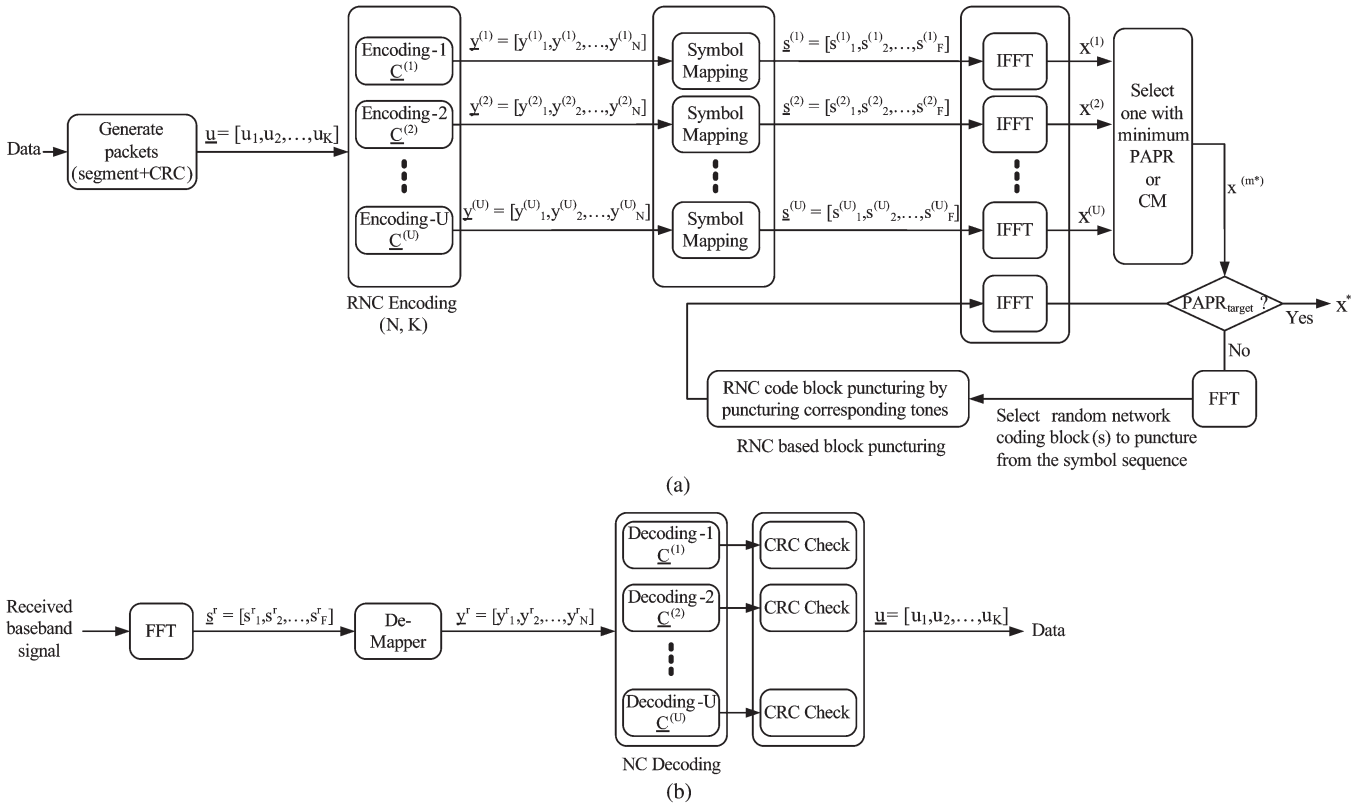

Fig. 1. Block diagram of the proposed PAPR reduction scheme using block-level RNC. (a) Block diagram of transmitter. (b) Block diagram of receiver.

the original K blocks by inverting the submatrix of coding coefficients corresponding to these K blocks.

Each generated coded block can be mapped to one or several modulation symbols. The required number of symbols for one coded block depends on the size of the coded block and the selected modulation scheme. For example, a coded block with a block size of 8 bits is mapped to four symbols for QPSK and two symbols for 16-QAM. Note that in this paper, we assume that the number N of coded blocks and their size should be determined so that they are loaded on the subcarriers of one OFDM symbol using the employed modulation level. For example, assuming a code rate of 1/2, 16-QAM, a block size of 8 bits, and 64 data subcarriers, the numbers of original and coded blocks should be set to $N = 32$ and $K = 16$, respectively. Thus, a 128-bit data segment is required to generate each original block vector.

To reduce the overhead of communicating coding coefficients between the transmitter and the receiver for each coded block, the coding coefficient matrices can be pregenerated and kept at the transmitter and receiver. These pregenerated coding matrices should have the ability to minimize the BLER. This design of coding matrices having such a property will be discussed in the next section.

B. Coefficient Matrix Generation

To design matrices that minimize the BLER, we adopt the following characteristic matrix concept from [23] and [26]:

$$\mathbf{C} = \mathcal{X}(\mathbf{A}) \quad : \quad \begin{cases} c_{ij} = 1, & \text{if } a_{ij} \neq 0 \\ c_{ij} = 0, & \text{if } a_{ij} = 0 \end{cases}$$

where a_{ij} and c_{ij} are the corresponding entries of matrices $\mathbf{A}$ and $\mathbf{C}$, respectively. To minimize the BLER, we use the following theorem that we proved in [23].

Theorem 1: For practical values of bit error rate on a channel, a coding matrix $\mathbf{A}$ achieves the minimum BLER and consequently maximum reliability iff its characteristic matrix $\mathbf{C} = \mathcal{X}(\mathbf{A})$ has the form

$$\mathbf{C} = \left[\mathbf{I}_K | \mathbf{E}_{K\times(N-K)}\right] \tag{9}$$

where $\mathbf{I}_K$ is the $K \times K$ identity matrix, and $\mathbf{E}_{K\times(N-K)}$ is the $K \times (N-K)$ all ones matrix.

To guarantee a successful decoding, any $K \times K$ submatrix of the coefficient matrix $\mathbf{A}$ should be nonsingular. The following theorem introduces a method to guarantee this property for $\mathbf{A}$ while obeying the condition in Theorem 1.

Theorem 2: The coefficient matrix $\mathbf{A}$ defined as

$$\mathbf{A} = \begin{pmatrix} 1 & 0 & \cdots & 0 & v_1 & v_2 & \cdots & v_{N-K} \\ 0 & 1 & \cdots & 0 & v_1^2 & v_2^2 & \cdots & v_{N-K}^2 \\ \vdots & \vdots & \ddots & \vdots & \vdots & \vdots & \vdots & \vdots \\ 0 & 0 & \cdots & 1 & v_1^K & v_2^K & \cdots & v_{N-K}^K \end{pmatrix}$$

satisfies the conditions of Theorem 1 and guarantees the nonsingularity of any K of its columns iff for $v_i \in GF(2^n)$, we have $v_i \neq v_j$, for $i, j \in \{1, \ldots, 2^n - 2\}$, where $2^n - 2 \geq N - K$.

Proof: The coefficient matrix $\mathbf{A}$ has a Vandermonde structure, and it is well known that a Vandermonde matrix has full rank unless if two columns are identical. Note that the two vectors $\underline{v}_1 = [v_1, v_1^2, \ldots, v_1^{n-1}]$ and $\underline{v}_2 = [v_2, v_2^2, \ldots, v_2^{n-1}]$,

with $v_1, v_2 \in GF(2^n)$ and $v_1 \neq v_2$, are linearly independent. This is due to the following facts:

1) For $x \in GF(2^n)$ and $x \neq 1$, the two terms x^{n_1} and x^{n_2} are not equal when $n_1 \neq n_2$, $n_1, n_2 \notin \{0, 1\}$, and $n_1, n_2 \leq n-1$.
2) For $x_1, x_2 \in GF(2^n)$ and $x_1, x_2 \neq 1$, the two terms x_1^i and x_2^i are not equal when $x_1 \neq x_2$ and $1 \leq i \leq n-1$.

Therefore, any $K \times K$ submatrix of $\mathbf{A}$ is nonsingular. ■

By combining available coefficient matrices, different coefficient matrices can be created to generate different OFDM transmit signals, as will be explained in the next section.

C. NC-SLM Scheme

Based on the foregoing coding procedures and coefficient matrix design, the original block vector $\underline{\mathbf{u}}$ is passed to U NC units, each using a realization of the coding matrix explained in Theorem 2. The output of these U units is U different vectors of coded blocks $[\underline{\mathbf{y}}^{(1)}, \underline{\mathbf{y}}^{(2)}, \ldots, \underline{\mathbf{y}}^{(U)}]$, each of size N blocks, from the original K blocks of $\underline{\mathbf{u}}$. Each coded block vector is mapped to a modulation symbol vector $\underline{\mathbf{s}}^{(m)} = [s_1^{(m)}, s_2^{(m)}, \ldots, s_F^{(m)}]$, where F is the number of data subcarriers, and $1 \leq m \leq U$. The length of each symbol $s_i^{(m)}$ is $Q = log_2(M)$, where M is the employed modulation level. After IFFT of these U candidate symbol streams into U candidate transmit signals $x^{(m)}$ $(1 \leq m \leq U)$, the transmitter selects the signal x^* with the lowest PAPR or CM for transmission or forwarding to the block puncturing step of our proposed scheme.

The U different coding matrices employed in the foregoing process can be preset and prestored in both transmitter and receiver. Consequently, the transmitter does not need to transmit the index of the selected coding matrix. Instead, the receiver tries to decode the received signal, after fast Fourier transform and symbol demapping, using the prestored U different matrices. After decoding the incoming bit sequence using these prestored U different matrices, the cyclic redundancy checks (CRCs) of the decoded frames are examined, and the frame that passes the CRC check is selected as the correctly received frame. If none of the decoded frames using U different matrices passes the CRC check, then the frame is discarded at the physical layer without delivering it to upper layers because this frame has errors. A similar strategy is employed for HARQ in various air interface standards, including IEEE 802.16 Worldwide Interoperability for Microwave Access and 3GPP LTE. Typically, the PAPR problem is a serious problem in the mobile station side because it requires good power amplifier. Therefore, PAPR reduction schemes are usually used in the uplink transmission. Since the base station, which is the receiver in the uplink transmission, has good computing capability, the base station can handle reasonable decoding complexity incurred by blind decoding.

The NC-SLM scheme uses U different coefficient matrices to generate symbol sequences, whereas the C-SLM scheme uses U different phase sequences to generate symbol sequences. To compare the complexity between NC-SLM and C-SLM, the differences between the two schemes should be investigated. As the number of subcarriers increases, the optimal SLM is NP-hard from the viewpoint of computational complexity theory. Since the optimization of SLM requires heavy computing complexity as the number of subcarriers increases, and the optimization of SLM is not our main objective of this paper, we utilized the original SLM scheme in [25] without optimization of phase sequences. For the same reason, our proposed scheme NC-SLM also does not optimize NC coefficient set search and employs schemes similar to C-SLM with difference of using NC. Therefore, the major difference is where multiplication operation takes place. For NC-SLM, multiplication operations are done at the bit level before symbol mapping. However, the multiplication operations in C-SLM take place at the symbol level after symbol mapping. Although NC-SLM adds a complexity of $U-1$ more symbol mappings than C-SLM, the complexity of the multiplication operation in NC-SLM is low.

According to the results in [27], a high-performance random NC can be implemented with the current processors. The coding speed could reach 1248 Mb/s for 16 blocks of 32 kB each and 348 Mb/s for 64 blocks of 32 kB each using the techniques in [27]. As our block size could be as small as a few bits (a block size of 8 bits is used in our NC operation), the encoding (multiplication) and decoding would be even much faster.

Algorithm 1 illustrates the summarized procedure of the NC-SLM algorithm. The processes in the FOR loop can be performed in parallel, as previously shown in Fig. 1.

Algorithm 1 NC-SLM Algorithm
Require: F, U, Q, r, n
SET *Operation field* to $GF(2^n)$
DIVIDE input bit streams into segments and append CRC to each segment, such that the size of the CRC appended segment is FQ
DIVIDE the segment into K blocks $\underline{\mathbf{u}} = [u_1, u_2, \ldots, u_K]$, each of size n
for $m = 1$ to U **do**
$\underline{\mathbf{y}}^{(m)} = \underline{\mathbf{u}} \times \mathbf{A}^{(m)}$
GENERATE its corresponding baseband representation signal, $x^{(m)}$ from (1)
CALCULATE $PAPR_m$ from (2) OR CM_m from (4) and (5)
end for
$m^* = \arg\min_m\{PAPR_m\}$ OR $m^* = \arg\min_m\{CM_m\}$
TRANSMIT $x^{(m^*)}$

IV. Block Puncturing

The block puncturing step is an additional step to our proposed scheme, which aims to further reduce PAPR or CM by iteratively finding and puncturing the blocks whose puncturing maximizes the PAPR or CM reduction. Block puncturing is equivalent to not loading the corresponding tones. For example, if the block size is 8 bits, and the first block is selected for puncturing in a 16-QAM–64-OFDM system, where 64 is the number of data subcarriers F, then the first two tones conveying the first block (two 16-QAM symbols) are not loaded with the

symbols corresponding to this block. Whereas punctured codes typically use less resources for transmission, the proposed block puncturing scheme does not reduce the resource used for transmission because the purpose of the proposed block puncturing scheme is to lower the PAPR.

Block puncturing is possible due to the design of our NC-SLM scheme. From (7), each transmitted block is a linear combination of the original blocks, and any combination of K transmitted blocks can reconstruct the original blocks. Since there is redundancy in the system, we can drop some of the blocks to reduce the PAPR while still being able to recover the original blocks. This step will indeed increase the BLER. However, if the resulting BLER is below the targeted value, then block puncturing is plausible.

The puncturing technique is widely used in channel coding, e.g., convolutional codes or turbo codes to make desired code rates. A PAPR reduction scheme using puncturing in turbo coded OFDM system, denoted as selected mapping–dynamic puncturing matrix (SLM-DPM), was proposed in [28]. SLM-DPM exploits punctured turbo codes and generates different turbo coded sequences by exploiting the puncturing matrix. After applying IFFT to these different code sequences, the coded sequence with the lowest PAPR is selected to transmit. Although SLM-DPM employs puncturing idea, our proposed scheme is much more flexible than SLM-DPM in terms of code rates. Whereas SLM-DPM cannot alter code rates, the proposed block puncturing PAPR reduction scheme can change code rates by exploiting the rateless property of NC. In addition, in comparison with the fact that the proposed block puncturing is utilized as an addition to the NC-SLM scheme, SLM-DPM is used as an SLM step to produce different coded sequences using punctured turbo codes.

The ability of block puncturing in reducing the PAPR can be justified using large deviation theory [29]. From (1), the instantaneous power of the OFDM symbol $x(t)$ at time t is given by

$$|x(t)|^2 = \sum_{i=1}^{F} |s_i|^2 + \sum_{i=1}^{F} \sum_{k=i+1}^{F} 2\Re\left\{s_i s_k^* \cdot \exp\left\{j2\pi(f_i - f_k)t\right\}\right\}, \quad 0 \le t \le T. \tag{10}$$

Let us define

$$\gamma_{ik}(y) = 2\Re\left\{s_i s_k^* \cdot \exp\left\{j2\pi(f_i - f_k)t\right\}\right\}. \tag{11}$$

Then, (10) can be written as

$$|x(t)|^2 = z(t) = \sum_{i=1}^{F} |s_i|^2 + \sum_{i=1}^{F} \sum_{k=i+1}^{F} \gamma_{ik}(t). \tag{12}$$

We assume that s_i and s_k are independent for $i \neq k$. Therefore, for very large values of F, the process $z(t)$ has the mixing property, which indicates that the theory of large deviation holds for $z(t)$. This claim can also be verified by noting that PAPR has a distribution with exponential tail (cf. Fig. 2). Using the theory of large deviation, we have

$$P\left(\max_t z(t) > \eta\right) \approx \max_t P\left(z(t) > \eta\right). \tag{13}$$

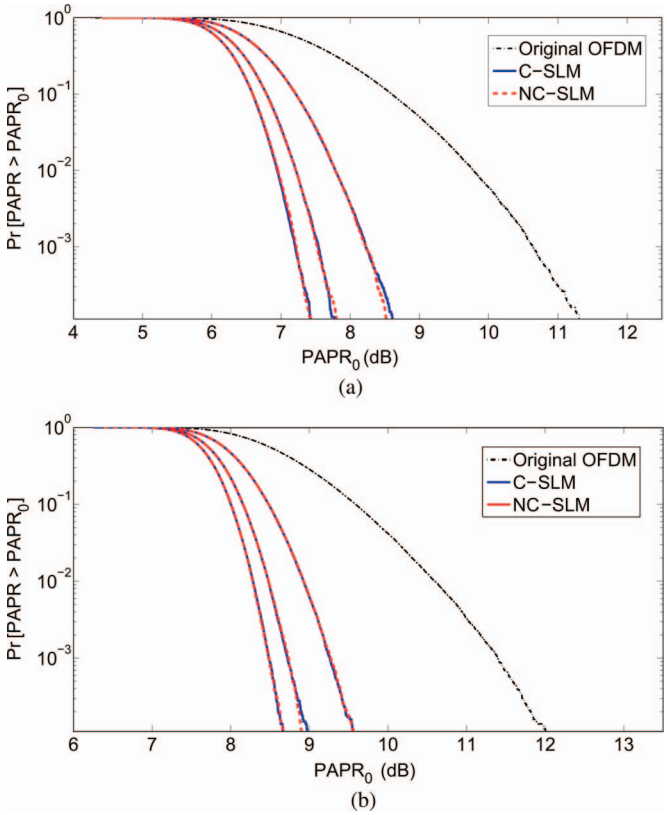

Fig. 2. PAPR CCDF performance of C-SLM and NC-SLM schemes without block puncturing for 16-QAM–OFDM signals. (a) $F = 64$ subcarriers. (b) $F = 512$ subcarriers.

Let $m = (F(F+1)/2)$ be the total number of terms in the summation (12). Using the Chernoff bound, we get

$$\max_t P\left(z(t) > \eta\right) = e^{-mI\left(\frac{\eta}{m}\right)} \tag{14}$$

where $I(.)$ is the rate function [29].

Block puncturing is performed by setting some of the s_i's equal to zero. Let $z_p(t)$ be the power of the induced signal at time instant t when the pth tone is punctured, that is,

$$|x_p(t)|^2 = z_p(t) = \sum_{\substack{i=1 \\ \neq p}}^{F} |s_i|^2 + \sum_{\substack{i=1 \\ \neq p}}^{F} \sum_{\substack{k=i+1 \\ \neq p}}^{F} \gamma_{ik}(t). \tag{15}$$

The total number of terms in the summation is $n = m - F$. Therefore, the Chernoff bound for $z_p(t)$ can be given by

$$\max_t P\left(z_p(t) > \eta\right) = e^{-nI\left(\frac{\eta}{n}\right)}. \tag{16}$$

Consequently

$$\frac{\max_t P\left(z_p(t) > \eta\right)}{\max_t P\left(z(t) > \eta\right)} = e^{-nI\left(\frac{\eta}{n}\right) + mI\left(\frac{\eta}{m}\right)}. \tag{17}$$

From the theory of large deviation, it is known that for $(\eta/m) > E[z(t)]$, the rate function is a convex increasing function of its argument. Given that $n < m$, we have $nI(\eta/n) > mI(\eta/m)$, and therefore

$$\max_t P\left(z_p(t) > \eta\right) < \max_t P\left(z(t) > \eta\right). \tag{18}$$

In other words, puncturing results in PAPR reduction.

In the foregoing analysis, we have assumed that the average power does not change after puncturing. In practice, since the maximum power tones are usually removed, the average power is also reduced. However, since the average power changes linearly while the maximum power changes exponentially, the effect of the latter factor is more substantive.

A. Selection of Punctured Blocks

Punctured blocks are selected in an iterative procedure. During the first iteration, one of the N coded blocks is punctured at a time, and the PAPRs/CMs of the resulting signals are measured and compared. Let $x_j(t)$ $(1 \le j \le N)$ be the signal (after IFFT) having the jth block punctured. The corresponding PAPR (denoted by $PAPR_j$) can be formulated as

$$PAPR_j = \frac{\max_{0\le t\le T} |x_j(t)|^2}{\frac{1}{T}\int_0^T |x_j(t)|^2\, dt}. \tag{19}$$

Similarly, we can formulate the corresponding CM (denoted by CM_j) as

$$CM_j = \frac{RCM_j - RCM_{\text{ref}}}{K_{\text{CM}}} \tag{20}$$

where

$$RCM_j = 20\log\left(RMS\left(\left(\frac{|x_j(t)|}{RMS\left(x_j(t)\right)}\right)^3\right)\right). \tag{21}$$

After measurement and comparison of the PAPRs/CMs, the block j^* that must be punctured is chosen as follows:

$$j^* = \arg\min_j\{PAPR_j\} \quad \text{OR} \quad j^* = \arg\min_j\{CM_j\}. \tag{22}$$

After the actual puncturing of the j^*th block, the new signal $x_{j^*}(t)$ is used to find a next puncturing block (i.e., the previous iteration is reexecuted with $x_{j^*}(t)$ as input). These iterations continue until a predefined number of iterations N_p is reached.

The complexity of search in this step is $O([N - N_p + 1] \times N_p)$. However, N_p is recommended to be a small number considering the tradeoff between PAPR reduction efficiency and error correction performance degradation, as shown in Section V. Therefore, the complexity of the search for the punctured blocks is within practical limits.

When this step is executed at the transmitter, the receiver employs the same method described in the previous section for frame reception. Note that the transmitter does not need to inform the receiver of the punctured block locations since they can be identified at the receiver by energy detection. In the decoding process, the decoding scheme in [30] can be employed where the log likelihood ratio (LLR) values of bits are used to select correctly received blocks. NC blocks with low LLR values are excluded in the decoding process. Low energy symbols of punctured blocks result in low LLR values in the demodulation process. Thus, blocks with low LLR values are avoided in the decoding process. Obviously, good detection performance of punctured blocks could be achieved at high SNR since the LLR values of the other unpunctured blocks would not be high enough to distinguish punctured blocks in low SNR channel conditions.

An important point to note is that this puncturing process reduces the number of alternatives to decode the original K blocks, leading to higher effective code rate where the effective code rate is defined as the code rate calculated with the number of effective parity bits after puncturing. If N_p blocks are punctured, then the effective code rate r_e is $r_e = K/(N - N_p)$. Such coding capability degradation (effective code rate increase) leads to a performance degradation in terms of BLER. Consequently, the block puncturing step can be used as a supplementary procedure to acquire the desired PAPR or CM level if this desired level is not reached after completing the main NC-SLM algorithm (illustrated in Algorithm 1). In the next section, we will analyze the PAPR-BLER tradeoff to show how block puncturing impacts the effective code rate (BLER performance). Moreover, we will show in Section V that substantial gains can be achieved when the puncturing step is executed after Step 1, even with the puncturing of a small number of blocks. This results in only a minor degradation in the BLER performance.

Algorithm 2 illustrates the summarized procedure of the proposed block puncturing step.

Algorithm 2 Block Puncturing Step
Require: N_p
  COMPUTE $x^{(m^*)}$ from **Algorithm 1**
  $\mathcal{P} \leftarrow \varnothing$ ($\mathcal{P}$ is the set of punctured blocks)
  for $i = 1$ to N_p **do**
    for $j = 1$ to N **do**
      if $j \notin \mathcal{P}$ **then**
        PUNCTURE the jth block
        GENERATE its corresponding baseband representation signal, x_j from (1)
        CALCULATE $PAPR_j$ from (19) OR CM_j from (20) and (21)
        RESTORE jth block
      end if
    end for
    $j^* = \arg\min_j\{PAPR_j\}$ OR $j^* = \arg\min_j\{CM_j\}$
    PUNCTURE block j^*
    $x^* \leftarrow x_{j^*}$
    $\mathcal{P} \leftarrow \mathcal{P} \cup j^*$
  end for
  TRANSMIT x^*

B. PAPR-BLER Tradeoff

In this section, we analyze the BLER degradation resulting from block puncturing for PAPR reduction. At the physical layer, one symbol contains several bits, and different bit positions of a constellation point may have different bit error probabilities [31]. When the employed modulation level is M, the number of bits per symbol is $Q = \log_2 M$. Let P_M^q,

$q = 1, 2, \ldots, Q$, be the bit error probability of the qth bit. Thus, when the modulation level M is used, the block error probability P_{blk} of a block with size n bits can be formulated as

$$P_{\text{blk}} = 1 - \left(\prod_{i=1}^{Q} \left(1 - P_M^i\right) \right)^{\frac{n}{Q}}. \tag{23}$$

If the coefficient matrix $\mathbf{A}$ satisfies the conditions of Theorem 1, a block is lost if the subcarriers loaded with that block are lost and at least K blocks are not received correctly from the remaining $N-1$ blocks. The modified block error probability P'_{blk} can be expressed in terms of the original BLER P_{blk} as

$$P'_{\text{blk}} = P_{\text{blk}} \times \left(1 - \sum_{i=K}^{N-1} \binom{N-1}{i} (1 - P_{\text{blk}})^i P_{\text{blk}}^{N-1-i} \right). \tag{24}$$

When blocks are punctured, the modified block error probabilities can be formulated into two forms, depending on what kind of blocks are punctured. If the N_p punctured blocks are all from the $\mathbf{I}_K$ part of the coefficient matrix $([\mathbf{I}_K | \mathbf{E}_{K\times(N-K)}])$, because $P_{\text{blk}} = 1$ and there are $N - N_p - 1$ blocks, the punctured block can only be recovered with correctly received at least K blocks from $N - N_p - 1$ blocks. Therefore, when $N - N_p$ is denoted as N', the modified block error probability of the punctured block $P_{lo\_\mathbf{I}}$ is

$$P_{lo\_\mathbf{I}} = 1 - \sum_{i=K}^{N'-1} \binom{N'-1}{i} (1 - P_{\text{blk}})^i P_{\text{blk}}^{N'-1-i}. \tag{25}$$

If the N_p punctured blocks are all from the $\mathbf{E}_{K\times(N-K)}$ part of the coefficient matrix $([\mathbf{I}_K | \mathbf{E}_{K\times(N-K)}])$, a block is lost when the original block from $\mathbf{I}_K$ part is lost, and at least K blocks are not received correctly from the remaining $N - N_p - 1$ blocks. Therefore, when $N - N_p$ is denoted as N', the modified block error probability $P_{lo\_\mathbf{E}}$ is

$$P_{lo\_\mathbf{E}} = P_{\text{blk}} \times \left(1 - \sum_{i=K}^{N'-1} \binom{N'-1}{i} (1 - P_{\text{blk}})^i P_{\text{blk}}^{N'-1-i} \right). \tag{26}$$

We can clearly see from (25) and (26) that the BLER of puncturing blocks generated by the $\mathbf{E}_{K\times(N-K)}$ part is lower than the BLER of puncturing blocks generated by the $\mathbf{I}_K$ part. Therefore, it is recommended to puncture NC blocks generated by the $\mathbf{E}_{K\times(N-K)}$ part of the coefficient matrices.

V. Simulations

A useful metric to measure the effectiveness of PAPR reduction algorithms is the complementary cumulative distribution function (CCDF) of the PAPR, which is the probability that the PAPR of an OFDM symbol exceeds the threshold level $PAPR_0$, i.e.,

$$\text{CCDF}\left(\text{PAPR}\left(x(t)\right)\right) = Pr\left(\text{PAPR}(x(t)) > PAPR_0\right).$$

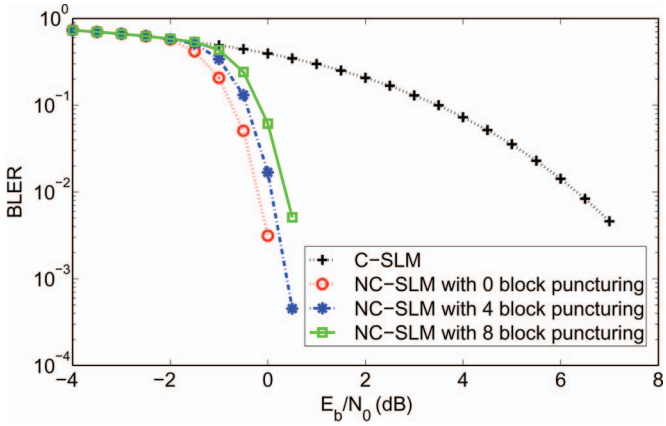

Fig. 3. BLER performance of C-SLM and NC-SLM (with/without block puncturing). The code rate of NC without puncturing is 1/2.

In [32], Sharif *et al.* showed that the oversampling rate greater than $\pi/\sqrt{(2)}$ can be tight bound such that the maximum of samples is a good representative of the maximum of the continuous time signal. Considering such bound, a high sampling rate, e.g., 8 for $F = 64$, is used in the simulations.

In the first simulation, PAPR is obtained using U (4, 8, and 12) different phase sequences and coefficient matrices for the C-SLM and the proposed NC-SLM schemes, respectively. Fig. 2 depicts the CCDF performance of the C-SLM and the proposed NC-SLM schemes for 64 and 512 data subcarriers when the algorithm is employed without block puncturing. In the simulation, data blocks fitting in one OFDM symbol are randomly generated, and the OFDM signal is obtained with 16-QAM symbol mapping and IFFT. With this setting, 100 000 OFDM signals are simulated, and the CCDF performance of PAPR is evaluated. The simulation results show that the proposed NC-SLM scheme achieves a performance similar to the C-SLM scheme. However, we should note that the same PAPR performance is achieved in NC-SLM with minimum BLER. Fig. 3 shows the BLER performance of C-SLM and NC-SLM (with or without block puncturing) under the additive white Gaussian noise channel condition. NC-SLM is able to achieve minimum BLER by employing the matrix form satisfying the conditions of Theorem 1 that was proved in [23]. The block puncturing of NC-SLM takes advantage of the rateless property of random NC: all the data blocks are encoded as a random linear combination of the original packets, and all the independent coded blocks are equally useful and innovative. Thanks to the rateless property of NC, the selection of different coefficient matrices and puncturing different blocks do not impact the performance of BLER as long as the number of punctured blocks is the same.

With the same simulation setting, we study the effect of block puncturing on PAPR. First, we use only block puncturing on the OFDM signal. Block puncturing is directly done on the OFDM signal without the NC-SLM step. Fig. 4 shows the CCDF of the block punctured signal for $N_p = 4$, 6, and 8 in the 64-subcarrier setting and $N_p = 8$, 16, and 32 in the 512-subcarrier setting, where N_p is the number of punctured blocks. As noticed, block puncturing is an effective method for PAPR reduction even without the use of the SLM technique.

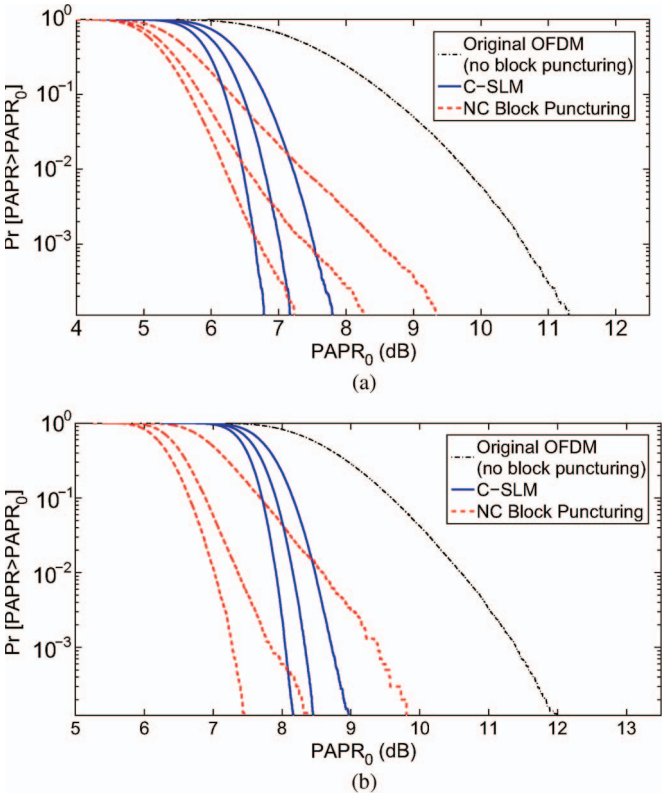

Fig. 4. PAPR CCDF performance of C-SLM and NC-SLM schemes with block puncturing for 16-QAM–OFDM signals (code rate without puncturing is 1/2). (a) $F = 64$ subcarriers. (b) $F = 512$ subcarriers.

We also plot the CCDF of the PAPR for the C-SLM algorithm in the figure. It is interesting to note that block puncturing can be more effective than SLM.

As noticed in the figure, the slope of the tail of CCDF decreases with the number of punctured blocks, which was predicted by the large deviation theory. Furthermore, when the number of data subcarriers increases, more coded block puncturing is required to achieve sufficient PAPR reduction (i.e., more blocks should be punctured for $F = 512$ as compared with $F = 64$). However, this increase in the number of punctured block does not affect the effective code rate. For example, when the code rate without block puncturing is 1/2, the effective code rate of four block puncturing in 64 subcarriers is the same as the effective code rate of 32 block puncturing in 512 subcarriers.

Fig. 5 compares the PAPR reduction that can be achieved by the NC-SLM scheme with block puncturing for different values of U. We can see that puncturing a small number of blocks can reduce the PAPR significantly.

To overcome the drawback of the PAPR metric, as identified in Section II, we evaluate our proposed scheme using the CM. With the same simulation setting of the 16-QAM–64-OFDM signal and for a code rate of 1/2, RCM is computed as described in Section II. The performance evaluation results of RCM are shown in Fig. 6. We can see that the proposed scheme also achieves a good performance when evaluated using the CM.

Fig. 7 depicts the BLER $P_{rmloss\_\mathbf{E}}$ performance as the number of punctured blocks increases for a 16-QAM–64-OFDM

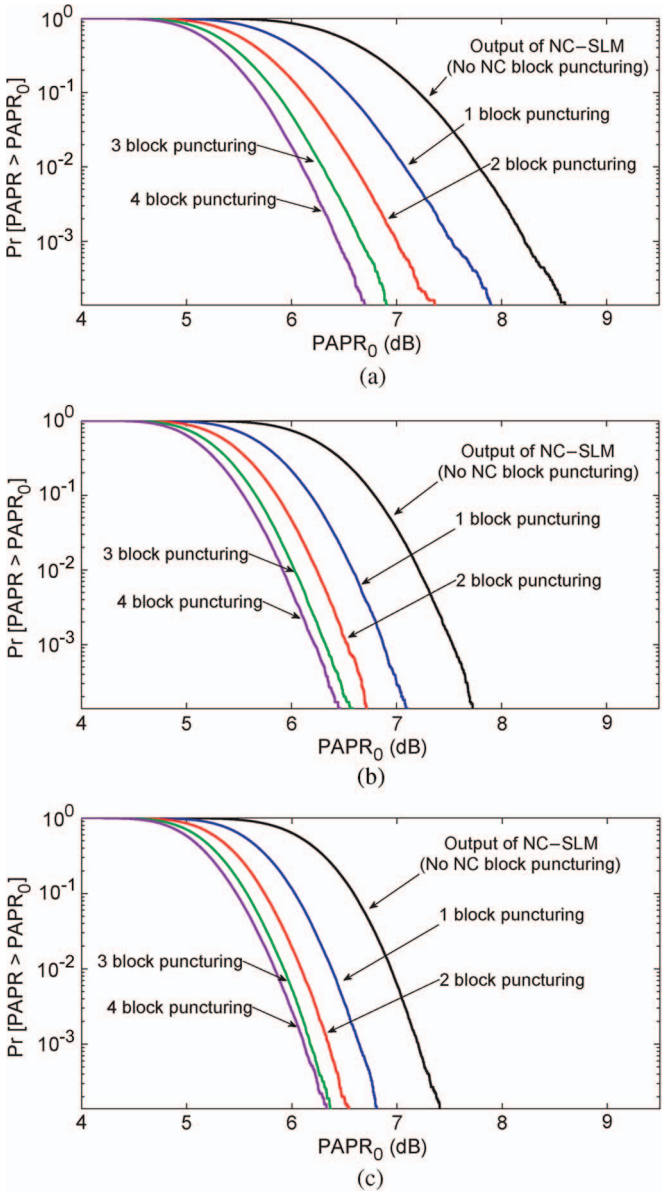

Fig. 5. PAPR CCDF performance of NC block puncturing as a second step after the NC-SLM step for 16-QAM–64-OFDM signals. (a) $U = 4$. (b) $U = 8$. (c) $U = 12$.

subcarrier system. Since C-SLM does not utilize NC, the BLER performance of C-SLM is not shown. "No NC block puncturing" can be regarded as outputs of NC-SLM with different NC rates. We can see that the BLER $P_{rmloss\_\mathbf{E}}$ increases with N_p, i.e., the number of punctured NC blocks. In the case of the code rate 1/2 without block puncturing, the effective code rates become 16/31 and 8/15 for $N_p = 2$ and 4, respectively. Similarly, for the code rate 1/4 without block puncturing, the effective code rates are 8/31 and 4/15 for $N_p = 2$ and 4, respectively. When the proposed block puncturing scheme is jointly used with the NC-SLM, a large PAPR reduction can be achieved even with few blocks puncturing.

Fig. 8 shows that the proposed block puncturing scheme achieves better PAPR reduction as the number of punctured blocks increases. However, the PAPR reduction gain achieved with block puncturing gets smaller and smaller as the number

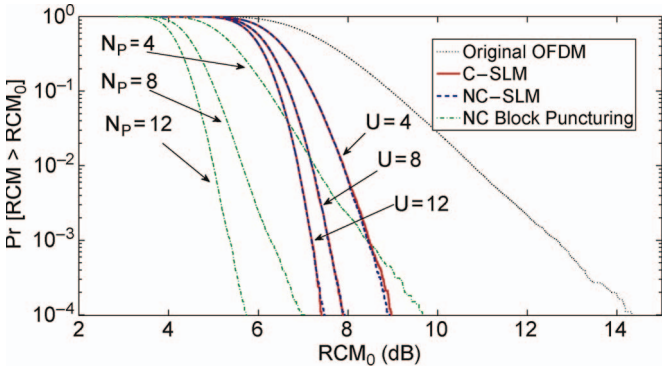

Fig. 6. CM performance for 16-QAM–64-OFDM signals (code rate without puncturing is 1/2).

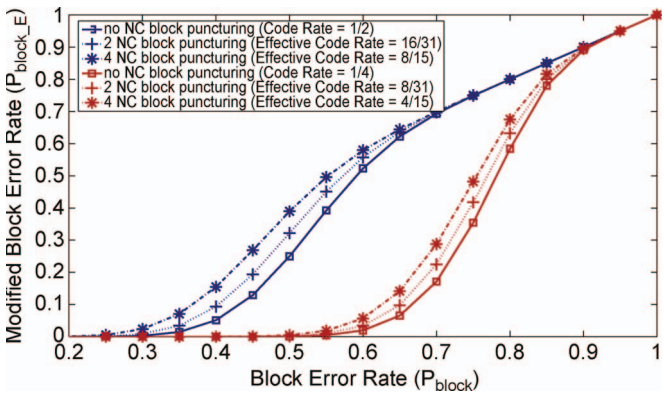

Fig. 7. BLER performance of block puncturing for 16-QAM–64-OFDM subcarrier signals. Code rate $= 1/2$ and 1/4 cases are used to show the modified BLERs with block puncturing.

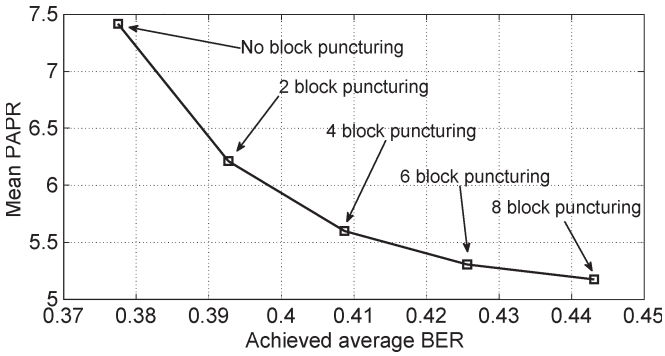

Fig. 8. Average BLER and PAPR (in decibels) relationship for 16-QAM–64-OFDM subcarrier signals.

of puncturing blocks increases. Therefore, the puncturing of the first few blocks is most efficient in terms of PAPR reduction.

VI. Conclusion

In this paper, we have explored the use of NC to jointly reduce PAPR/CM and BLER in multicarrier (OFDM) signals. The proposed scheme is able to work with both PAPR and CM. The proposed algorithm satisfies both the conditions required for achieving minimum BLER and reducing PAPR/CM simultaneously. By utilizing a favorable randomization property of NC, the proposed NC-SLM algorithm was introduced. Moreover, we proposed an NC block puncturing step on top of the proposed NC-SLM scheme for further PAPR/CM reduction.

Simulation results confirmed that the NC-SLM scheme already achieves the same PAPR reduction performance as the C-SLM. Adding the NC block puncturing step to the NC-SLM scheme makes it outperform the C-SLM PAPR reduction scheme. We also showed the effect of block puncturing on the BLERs. Simulations also showed that substantial PAPR/CM reduction gains can be achieved with puncturing a few blocks (as few as one block). Thus, the impact of block puncturing on the BLER is minor. Moreover, we suggested the use of the NC block puncturing as a supplementary step if the desired PAPR/CM is not achieved by the NC-SLM. By utilizing the proposed scheme, mobile devices will be able to enjoy both the benefits of NC in multicarrier systems and the reduction of PAPR, which allows better use of power amplifiers.

Acknowledgment

This paper is an extension of our paper [1] published in ICC 2009.

References

[1] A. A. Yazdi, S. Sorour, S. Valaee, and R. Y. Kim, "Joint reduction of peak to average power ratio and symbol loss rate in multicarrier systems," in *Proc. IEEE ICC*, Jun. 2009, pp. 1–5.

[2] Y. Lee, E. Lee, I. Song, S. Y. Kim, and S. Yoon, "A new pilot-aided integer frequency offset estimation method for digital video broadcasting (DVB) systems," in *Proc. ICACT*, Feb. 2008, pp. 1694–1696.

[3] Wireless LAN Medium Access Control (MAC) and Physical Layer (PHY) Specifications, ANSI/IEEE 802.11, 1999.

[4] IEEE Standard for Local and Metropolitan Area Networks, Part 16: Air Interface for Fixed and Mobile Broadband Wireless Access Systems, IEEE Std. 802.16e-2005, Dec. 2005.

[5] K. C. Beh, A. Doufexi, and S. Armour, "Performance evaluation of hybrid ARQ schemes of 3GPP LTE OFDMA system," in *Proc. PIMRC*, Sep. 2007, pp. 1–5.

[6] 3GPP TSG RAN WG4 #31,3GPP TSG RAN WG1 #37, Motorola Tdoc R4-040367, R1-040522 and R1-040642 Comparison of PAR and cubic metric for power derating2004, May.

[7] 3GPP TSG RAN WG1 LTE, Motorola Tdoc R1-060023 Cubic metric in 3GPP-LTE2006, Jan..

[8] H. Ochiai and H. Imai, "Performance analysis of deliberately clipped OFDM signals," *IEEE Trans. Commun.*, vol. 50, no. 1, pp. 89–101, Jan. 2002.

[9] C. Kikkert, "Digital companding techniques," *IEEE Trans. Commun.*, vol. COM-22, no. 1, pp. 75–78, Jan. 1974.

[10] R. Raich, H. Qian, and G. T. Zhou, "Optimization of SNDR for amplitude-limited nonlinearities," *IEEE Trans. Commun.*, vol. 53, no. 11, pp. 1964–1972, Nov. 2005.

[11] J. Tellado, L. M. C. Hoo, and J. M. Cioffi, "Maximum likelihood detection of nonlinearly distorted multicarrier symbols by iterative decoding," *IEEE Trans. Commun.*, vol. 51, no. 2, pp. 218–228, Feb. 2003.

[12] A. E. Jones, T. A. Wilkinson, and S. K. Barton, "Block coding scheme for reduction of peak to mean envelope power ratio of multicarrier transmission schemes," *Electron. Lett.*, vol. 30, no. 25, pp. 2098–2099, Dec. 1994.

[13] M. Breiling, S. H. Muller-Weinfurtner, and J. B. Huber, "SLM peak-power reduction without explicit side information," *IEEE Commun. Lett.*, vol. 5, no. 6, pp. 239–241, Jun. 2001.

[14] L. J. Cimini, Jr. and N. R. Sollenberger, "Peak-to-average power ratio reduction of an OFDM signal using partial transmit sequences," *IEEE Commun. Lett.*, vol. 4, no. 3, pp. 86–88, Mar. 2000.

[15] J. Tellado, "Peak to average power reduction for multicarrier modulation," Ph.D. dissertion, Stanford Univ., Stanford, CA, 2000.

[16] B. S. Krongold and D. L. Jones, "PAR reduction in OFDM via active constellation extension," *IEEE Trans. Broadcast.*, vol. 49, no. 3, pp. 258–268, Sep. 2003.

[17] R. J. Baxley, "Analyzing selected mapping for peak-to-average power reduction in OFDM," Ph.D. dissertation, Georgia Inst. Technol., Atlanta, GA, May, 2005.
[18] A. D. S. Jayalath and C. Tellambura, "A blind SLM receiver for PAR-reduced OFDM," in *Proc IEEE VTC*, Sep. 2002, vol. 1, pp. 219–222.
[19] P. Eevelt, M. Wade, and M. Tomlinson, "Peak to average power reduction for OFDM schemes by selective scrambling," *Electron. Lett.*, vol. 32, no. 21, pp. 1963–1964, Oct. 1996.
[20] S. Lin and D. J. Costello, *Error Control Coding: Fundamentals and Applications*. Englewood Cliffs, NJ: Prentice-Hall, 1983.
[21] R. Ahlswede, N. Cai, S. R. Li, and R. W. Yeung, "Network information flow," *IEEE Trans. Inf. Theory*, vol. 46, no. 4, pp. 1204–1216, Jul. 2000.
[22] J. Jin, B. Li, and T. Kong, "Is random network coding helpful in WiMAX?" in *Proc. IEEE INFOCOM*, 2008, pp. 2162–2170.
[23] A. A. Yazdi, S. Sorour, S. Valaee, and R. Y. Kim, "Optimum network coding for delay sensitive applications in WiMAX unicast," in *Proc. IEEE INFOCOM*, Apr. 2009, pp. 2576–2580.
[24] S. Katti, D. Katabi, H. Balakrishnan, and M. Medard, "Symbol-level network coding for wireless mesh networks," in *Proc. ACM SIGCOMM*, 2008, pp. 401–412.
[25] R. Bauml, R. Fischer, and J. Huber, "Reducing the peak-to-average power ratio of multicarrier modulation by selected mapping," *Electron. Lett.*, vol. 32, no. 22, pp. 2056–2057, Oct. 1996.
[26] A. A. Yazdi, S. Sorour, S. Valaee, and R. Y. Kim, "Reducing symbol loss probability in the downlink of an OFDMA based wireless network," in *Proc. ICC*, May 2008, pp. 3485–3489.
[27] H. Shojania and B. Li, "Parallelized progressive network coding with hardware acceleration," in *Proc. 15th IWQoS*, 2007, pp. 47–55.
[28] C. Zhao, G. Wei, and J. K. Zhu, "SLM-DPM scheme for PAR reduction in TC-OFDM system," in *Proc. IEEE VTC*, May 2004, pp. 1765–1767.
[29] A. Dembo and O. Zeitouni, *Large Deviation Techniques and Applications*., 2nd ed. New York: Springer-Verlag, 1998, ser. Application of Mathematics.
[30] R. Y. Kim, J. Jin, and B. Li, "Drizzle: Cooperative symbol-level network coding in multi-channel wireless networks," *IEEE Trans. Veh. Technol.*, vol. 55, no. 3, pp. 1415–1432, Mar. 2010.
[31] M. P. Fitz and J. P. Seymour, "On the bit error probability of QAM modulation," *Int. J. Wireless Inf. Netw.*, vol. 1, no. 2, pp. 131–139, Apr. 1994.
[32] M. Sharif, M. Gharavi-Alkhansari, and B. H. Khalaj, "On the peak-to-average power of OFDM signals based on oversampling," *IEEE Trans. Commun.*, vol. 51, no. 1, pp. 72–78, Jan. 2003.

Ronny Yongho Kim (M'06–SM'10) received the B.S. degree from Inha University, Incheon, Korea, and the M.S. and Ph.D. degrees from Yonsei University, Seoul, Korea, in 2004 and 2010, respectively.

From 1998 to 2010, he was a Senior Research Engineer with LG Electronics, where he was working on the research and standardization of future wireless technologies, primarily within the area of medium-access control (MAC) and network protocol design. Since 2010, he has been with the School of Computer Engineering, Kyungil University, Gyeongsan, Korea, where he is currently an Assistant Professor. He has actively participated in IEEE 802.16, IEEE 802.11, and IEEE 802.21, and made significant contributions. From 2005 to 2006, he served as the Liaison Official between the IEEE 802.16 and IEEE 802.21 working groups. His current research interests are wireless networks, mobility management, power-efficient protocols, IT convergence, machine-to-machine communications, and network coding.

Young Yong Kim (M'98) received the B.S. and M.S. degrees from Seoul National University, Seoul, Korea, in 1991 and 1993, respectively, and the Ph.D. degree from the University of Texas, Austin, in 1999.

From 1998 to 2000, he was a Research Scientist with the Wireless Network Management Research Group, Telcordia Technologies (formerly Bell Communication Research), Red Bank, NJ. Since 2000, he has been with Yonsei University, Seoul, where he is currently an Associate Professor in the Department of Electrical and Electronic Engineering. His interests include wireless channel modeling, performance evaluation of mobile networks, and design and analysis of multimedia wireless systems.

Amin Alamdar Yazdi (S'08) received the B.Sc. degree in electrical engineering in 2006 from Sharif University of Technology, Tehran, Iran, and the M.A.Sc. degree in 2008 from the University of Toronto, Toronto, ON, Canada, where he is currently working toward the Ph.D. degree.

His research interests include coding theory, wireless communications, and low-complexity algorithms.

Sameh Sorour (S'98) received the B.Sc. and M.Sc. degrees in electrical engineering from Alexandria University, Alexandria, Egypt, in 2002 and 2006, respectively, and the Ph.D. degree from the University of Toronto, Toronto, ON, Canada.

In 2002, he was with the Department of Electrical Engineering, Alexandria University, where he was a Teaching and Research Assistant for three years and was promoted to Assistant Lecturer in 2006. He is also served as the Chair of local arrangements for IEEE PIMRC 2011. He is currently a Postdoctoral Fellow with the University of Toronto. His research interests include opportunistic, random, and instantly decodable network coding applications in wireless networks, vehicular and high speed train networks, indoor localization, adaptive resource allocation, OFDMA, and wireless scheduling.

Shahrokh Valaee (S'88–M'00–SM'02) received the B.Sc. and M.Sc. degrees in electrical engineering from Tehran University, Tehran, Iran, and the Ph.D. degree from McGill University, Montreal, QC, Canada.

From 1994 to 1995, he was a Research Associate with INRS Telecom, University of Quebec, Quebec City, QC, Canada. From 1996 to 2001, he was an Assistant Professor with the Department of Electrical Engineering, Tarbiat Modares University, Tehran, and the Department of Electrical Engineering, Sharif University of Technology, Tehran. Since 2001, he has been a faculty member with the Edward S. Rogers Sr. Department of Electrical and Computer Engineering, University of Toronto, Toronto, ON, Canada, where he is the Associate Chair for Undergraduate Studies, holds the Nortel Institute Junior Chair of Communication Networks, and is the Director of the Wireless and Internet Research Laboratory (WIRLab). His current research interests are in wireless vehicular and sensor networks, location estimation, and cellular networks.

Dr. Valaee is an Editor of the IEEE TRANSACTIONS ON WIRELESS COMMUNICATIONS and an Associate Editor of IEEE SIGNAL PROCESSING LETTERS. He is the TPC Co-Chair and the Chair of the Organizing Committee of the 2011 IEEE International Symposium on Personal, Indoor and Mobile Radio Communications (PIMRC). He was the Co-Chair for the Wireless Communications Symposium of the 2006 IEEE Global Telecommunications Conference (GLOBECOM), a Guest Editor for the IEEE WIRELESS COMMUNICATIONS Magazine, a Guest Editor for the Wiley *Journal on Wireless Communications and Mobile Computing*, and a Guest Editor of EURASIP *Journal on Advances in Signal Processing*.